ELSEVIER

Journal of Nuclear Materials 266–269 (1999) 546–551

journal of nuclear materials

Space resolved fluctuations of electron density measured by means of two thermal Li-beams in TEXTOR-94

A. Huber [a,*], A.V. Nedospasov [b], U. Samm [a], B. Schweer [b]

[a] *Institut für Plasmaphysik, Forschungszentrum Jülich GmbH, EURATOM Association, Trilateral Euregio Cluster, D-52425 Jülich, Germany*

[b] *Institute of High Temperatures, Russian Academy of Sciences, Moscow, Russian Federation*

Abstract

Fluctuations of the electron density have been investigated in the edge of the tokamak TEXTOR-94 using two thermal Li-beams. Both the *radial* and *poloidal* correlation functions and their corresponding correlation lengths have been investigated inside and outside the last closed flux surface (LCFS) simultaneously. These measurements show considerable differences between the fluctuation properties on open and closed fieldlines. At all conditions the results indicate that the poloidal correlation length is a factor of 3 to 4 larger than the radial correlation length. The dependence of the fluctuation parameters on various discharge conditions is presented.

Keywords: Beam probe spectroscopy; Edge plasma; Fluctuations; Turbulence

1. Introduction

Plasma turbulence is considered to be an important factor influencing particle and heat transport in the tokamak periphery. However, the instability mechanisms and the control of the fluctuations are not yet clarified completely. An improved knowledge of the temporal–spatial structure of fluctuations is a prerequisite for a deep comprehension of their nature. An extensive study of the spatial structure of fluctuations was performed in the CALTECH [1] and ASDEX [2] tokamaks and in the W7-AS stellarator [3]. Investigations of fluctuations with *radial* resolution have also been performed on TEXTOR [4] using the thermal Li-beam. Generally it was found that the fluctuation structures are extended along the magnetic field while they are poloidally and radially localized within a few centimeters. A new diagnostical set-up for the *simultaneous measurement of radial and poloidal* components of fluctuation parameters has been installed in TEXTOR-94 using the spectroscopic observation of two thermal Li-beams. This method can be operated continuously over long discharges without disturbance of the plasma and without restriction to heat load.

2. Experimental arrangement

The investigation of plasma turbulence in the edge has been performed in the tokamak TEXTOR-94 at the following discharge parameters: $B_T = 2.25$ T, $I_p = 350$ kA, $R = 1.75$ m, $a = 0.46$ m, $\bar{n}_e = (1-4) \times 10^{19}$ m^{-3} in both ohmically and beam heated discharges. A simultaneous determination of the radial and poloidal components of fluctuation parameters was achieved by the operation of two narrow Li-beams (FWHM $\approx$ 10 mm), which were separated by 50 mm. The beams of thermal Li-atoms have been generated by a newly developed oven, which provides a long operation time and a high reliability. The Li-atoms with a mean velocity of ≈ 1.7 km/s were injected radially into the plasma edge, where they were excited and ionized by the plasma. The line radiation at $\lambda = 670.8$ nm of the excited atoms was observed, usually used for determination of electron

* Corresponding author. Tel.: +49 2461 61 2631; fax: +49 2461 61 2660; e-mail: a.huber@fz-juelich.de

0022-3115/99/$ – see front matter
PII: S0022-3115(98)00672-2

density profiles [5,6]. These measurements were performed with high temporal ($\Delta t \simeq 2$ μs) and spatial resolution ($\Delta_r \simeq 1$ mm in radial and $\Delta_p \simeq 10$ mm in poloidal direction), thus allowing also the determination of fluctuations from $\tilde{I}/I$, where I and $\tilde{I}$ are the local photon emission and its fluctuation, respectively.

The double oven was mounted on top of TEXTOR-94 and the observation range of the detection system was between $r = 440$ mm and $r = 500$ mm. Depending on the rotation angle of the system the beams can be separated in poloidal and toroidal direction. The latter one does not affect the measurement, because the correlation length along the magnetic field line is very long [7]. However, the toroidal separation is necessary to allow the observation of the two beams. By rotating the double oven, the poloidal distance between the two beams can be changed within steps of $\Delta\alpha = 3.75°$.

The line radiation due to the interaction between Li-atoms and electrons was imaged with a lens onto two arrays with 16 light guides connected to photomultipliers (Fig. 1). Each array consists of 8 channels (light guides) arranged in radial direction and collects the emission light from one beam. The centers of the light guides are 2 mm apart from each other so that the entire arrangement covers about ≈ 17 mm in radial direction. Both arrays can be moved in radial direction. Due to this possibility, the whole Li_{2p-2s}-emission profile can be measured with a fast detection system. For spatial analysis of the turbulence structure we have used the normalized cross-correlation functions $cor(x,\tau) = \int_{-\infty}^{\infty} f(t)g(t+\tau)\mathrm{d}t / \int_{-\infty}^{\infty} f(t)g(t)\mathrm{d}t$, and the correlation length l is defined in this work as $cor(l,0) = 1/e$. The radial distribution of the Li-emission line is measured with a 2d-camera with 128×128 elements every 20 ms (slow system). The radial profiles of n_e can be deduced from this emission signals. The combination of measurements with photomultiplier and 2d-camera allows the determination of the absolute density fluctuation $\tilde{n}_e$.

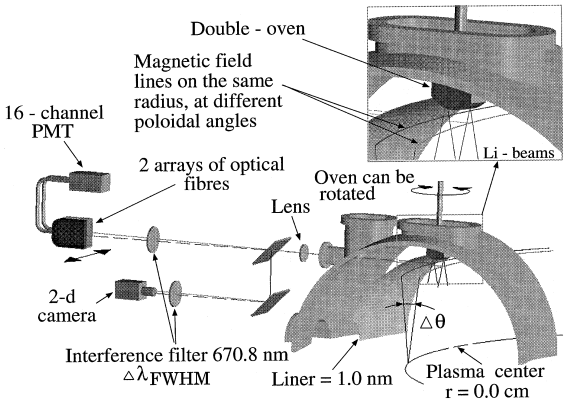

Fig. 1. Observation system of the Li-beam diagnostic at TEXTOR-94.

More details about the experimental set-up are given in [8,9].

3. Results

The radial variation of the relative fluctuation amplitudes in radial range of $r = 400$–500 mm is presented in Fig. 2. The measurements were made in a series of three ohmic discharges with the same plasma parameters ($\overline{n}_e = 1.5 \times 10^{19}$ m^{-3}). The relative error due to photon statistics was ≈ 2%. A continuous increase of the relative amplitudes $\tilde{n}_e/n_e$ with higher plasma radii can be seen: from about 8% on the LCFS up to about 20% at $r = 500$ mm. The absolute amplitude of the fluctuations is calculated from the mean value of electron density and the relative fluctuation amplitudes, showing an increase with smaller radii (Fig. 2).

An important parameter of fluctuations is the spatial extent of fluctuation events, presented by the radial and poloidal correlation length. Fig. 3 shows the typical radial correlation length l_r found on TEXTOR-94. The correlation length is presented as a function of $\overline{n}_e$ for ohmic discharges and for discharges with neutral beam heating (NBI). These measurements were carried out at a plasma radius of $r = 466$ mm. We see that the correlation length with NBI–heating is larger than with ohmic heating alone in the range of $\overline{n}_e = (1.0 - 4.0) \times 10^{19}$ m^{-3}. The increase of the radial correlation length with heating power has also been observed in the DIII-D tokamak [10]. Cooling by neon injection to achieve a large radiation level γ in discharges with NBI-heating leads to an additional increase of l_r.

Fig. 4 shows the relation of l_r/λ_n as function of the measured fluctuation level, where λ_n is the e-folding length of the electron density. The density fluctuations can be aproximated by $\tilde{n}_e/n_e \sim 0.25 \times l_r/\lambda_n$, which is

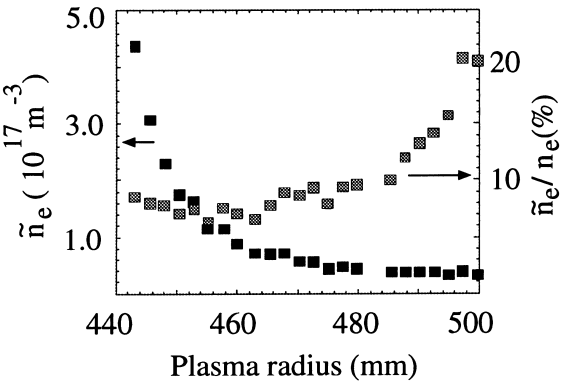

Fig. 2. Radial variation of the relative and absolute fluctuation amplitudes of electron density. The limiter was located at the plasma radius $r = 460$ mm.

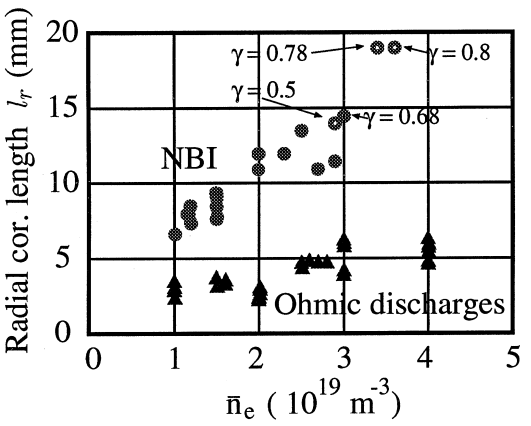

Fig. 3. Radial correlation lengths as function of $\bar{n}_e$ at plasma radius $r = 466$ mm: the triangles represent discharges with ohmic heating; dots discharges with additional neutral beam heating; circles discharges with neutral beam heating and neon injection, where $\gamma = P_{rad}/P_{heat}$ is the ratio between total radiated power and total heating power.

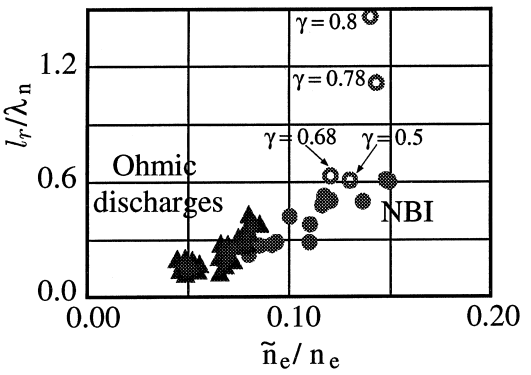

Fig. 4. l_r/λ_n versus relative electron density fluctuation $\tilde{n}_e/n_e$.

consistent with the *mixing length estimation* within a factor of 4. This is valid for small fluctuation wavelengths $\lambda \ll \lambda_n$ and correspondingly for $l_r \ll \lambda_n$. For discharges with neon this estimation is not valid since $l_r/\lambda_n \gtrsim 1$. The fluctuation levels in discharges with NBI are higher than in pure ohmic discharges.

Fig. 5 (left, top) shows the radial correlation function for an ohmic discharge. The measurement range was *outside* the LCFS between 468 mm and 482.4 mm. The plasma radius of the reference signal r_B was 475.2 mm. The level of the correlation function is drawn by equidistant lines. The degree of correlation is coded in a color scale (red maximum, blue minimum). This figure shows a 'correlation structure' which is extended along a straight line. The inclination of this structure gives the velocity of the fluctuations in radial direction: $v_r \approx 1.4 \times 10^2$ m/s. The sign of the inclination indicates that the velocity is directed inward.

Due to poloidal separation of the two beams, the poloidal and radial correlation functions can be determined simultaneously. Fig. 5 (right, top) shows the cross-correlation for six poloidal separations at the plasma radius of $r = 475$ mm. To achieve this, the same number of identical discharges was needed. The poloidal angle between the beams was changed after every discharge.

This presentation shows, that the maximum of correlation varies with the poloidal separation. This can be explained by a propagation velocity of the fluctuations. The inclination of the correlation shape gives a poloidal velocity of $v_\theta \approx 10^3$ m/s. The direction of the motion can be determined from the sign of time delay. The fluctuations propagate in the diamagnetic drift direction of the ions.

The poloidal correlation length is a factor of 3 to 4 larger than the radial correlation length. Fig. 5 (bottom) shows the radial and poloidal correlation functions *inside* the LCFS. All measurements were carried out under the same plasma conditions. We observe that the fluctuations move inside the LCFS in opposite direction: poloidally in the direction of the electron diamagnetic drift, radially outwards.

The radial and poloidal correlation functions provide the radial and poloidal components of the propagation velocity of fluctuation. It cannot be decided whether the observed velocity were bulk velocities of plasma or velocities of fluctuation, or any combination of both. The poloidal drift velocity of the plasma, $\rightarrow v_\theta \sim {}_r \times$, measured by a fast reciprocating probe located at the midplane of TEXTOR-94 is about 1 km/s outside LCFS [11] and of the same order as the poloidal propagation velocity of fluctuations determined from the correlation analysis presented here. The ${}_r \times$-velocity is able to contribute an essential part to the poloidal and radial propagation velocity. Let us consider, for example, a plane wave with wave number and phase velocity $\rightarrow v_\theta$ directed radially outwards. If the plasma has such a poloidal velocity $\rightarrow v_\theta$ that the projection of this velocity on the -direction is larger than the phase velocity $(\rightarrow v_\theta - \rightarrow v k_r/k) > 0$, one sees the inverted figure, the wave moves inwards.

Experiments with different magnetic field direction have been made to examine the influence of rotation. Fig. 6 shows the radial correlation function for two different cases: normal field configuration ($I_p \uparrow\downarrow B_t$) (top) and inverted configuration ($I_p \uparrow\uparrow B_t$) (bottom). The measurements were carried out in two ohmic discharges with identical plasma parameters ($\bar{n}_e = 2.5 \times 10^{19}$ m^{-3}). We observe that the fluctuations with inverted magnetic field propagate in the opposite direction. At the normal configuration the fluctuations propagate with a radial velocity of $\approx 10^2$ m/s inwards and with reversed magnetic field it moves with radial velocity of $\approx 2 \times 10^2$ m/s outwards. The lifetime of the fluctuations is in both

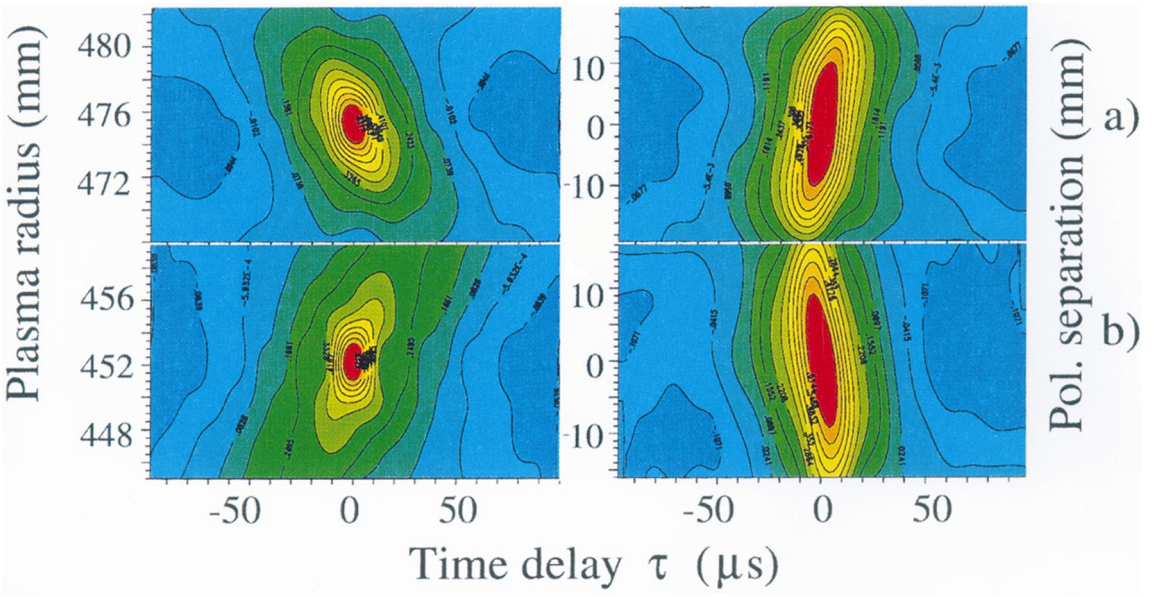

Fig. 5. Radial (left) and poloidal (right) correlation functions (a) outside the LCFS [top], (b) inside the LCFS [bottom].

cases approximately the same ($\tau_{life} \approx 30$ μs). The half width of the auto-correlation functions are different. This can be explained by different radial components of the propagation velocity. The auto-correlation function is narrow at large velocities.

Fig. 7 shows the poloidal correlation functions for these two cases, which were received from two poloidally displaced points. The correlation in the case $I_p \uparrow\downarrow B_t$ has a maximum during negative time delay. The maximum of correlation with inverted magnetic field is located at positive time delay. This fact can be explained by different rotation directions. The fluctuations propagate in both cases in the direction of the ion diamagnetic drift: electron and ion diamagnetic drift directions are inverted when B is inverted. In the normal field configuration the electrons drift to the top of the plasma column. The ions drift to the bottom. One observes a change of the poloidal distance between the measurement points and a

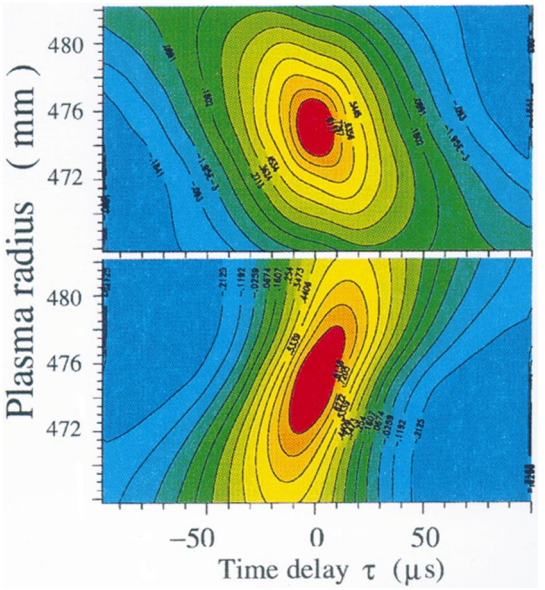

Fig. 6. Radial correlation functions with different magnetic field directions: B_t and I_p antiparallel (top) and B_t and I_p parallel (bottom).

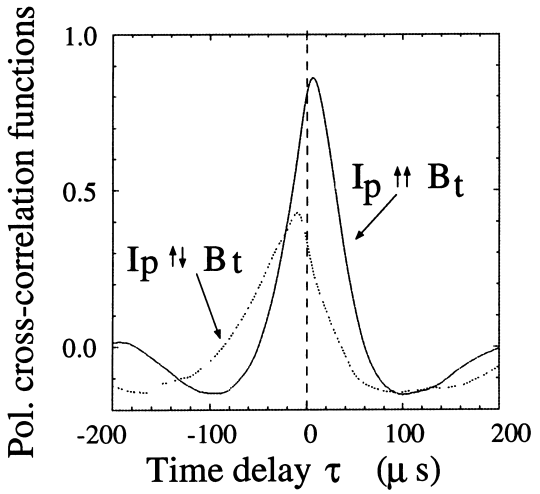

Fig. 7. The poloidal correlation functions with different magnetic field directions.

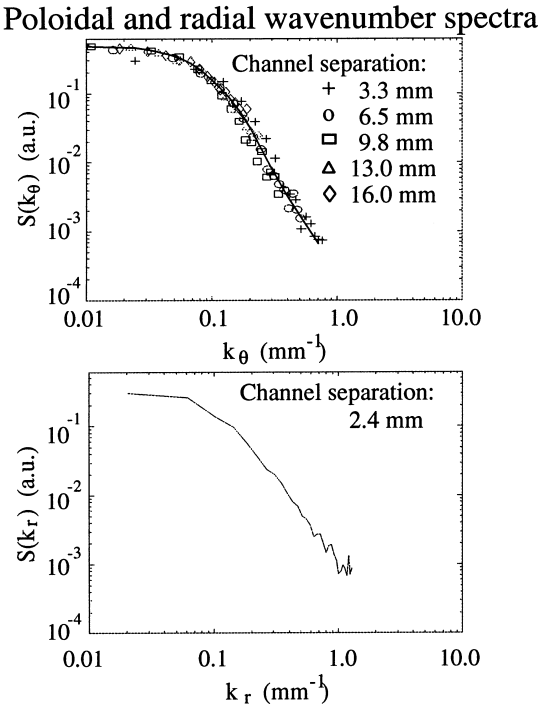

Fig. 8. Radial (bottom) and poloidal (top) wave number spectrum outside the last closed flux surface.

corresponding different values of the correlation functions due to the helicity of the magnetic field. The poloidal correlation functions shown in Fig. 7 differ by a factor of about 2.

An integration of frequency and wave number spectra $S(k,\omega)$ over the frequencies yields the typical $S(k)$ dependence shown in Fig. 8. At large k we have $\tilde{n}_e^2 \sim k^{-q}$. In our experiments with $\bar{n}_e = 1.5 \times 10^{19}$ m^{-3} $q \approx 3 - 3.2$ for poloidal waves and $q \approx 2.2 - 2.4$ for radial waves.

4. Discussion

4.1. Distribution of the density oscillations over the spectrum of the turbulence.

In many papers [12–15], it was shown that the theories of interchange turbulence in the scrape-off layer (SOL) with dissipation by currents flowing through the potential sheath near the surface (SD-surface dissipation) are usually capable to explain the experimental data. Pressure perturbations cause perturbations in the current to the limiter which, in turn, vary the potential distribution and cause a fluctuation of the poloidal electric field. In this case, a positive pressure perturbation shifts towards domains with lower pressure, i.e. a convective instability exists.

The mechanical work due to plasma expansion in its turbulent motion in the radial direction is dissipated by a fluctuating current near the surface

$$\int_V \upsilon \bigtriangledown \mathrm{pdV} = -\int_S (j_\parallel \phi)\mathrm{d}S. \tag{1}$$

Here ϕ is the plasma potential, υ the mean plasma velocity. Due to the surface dissipation the energy is transmitted from one wave to others. Since the fluctuations in the SOL are correlated over some short transverse dimensions, the dissipation of energy is also local in the range of the correlation scale, independent of the oscillations beyond this scale. According to the experimental data obtained with Langmuir probes, the fractal dimensionality of the random oscillations in the SOL varies in the range of 6–16, i.e. they are sustained by the interaction of a small number of independent modes [16]. This circumstance was used in [17] for the first approximation of the turbulence spectrum. The dependence of the level of fluctuations on the waves numbers can be estimated more easily with the assumption that an individual non-linear wave is local (i.e. it does not exchange energy with other waves). The level of the relative fluctuations, which are responsible for dissipation in the wall layer (this dissipation limits the growth of the wave), varies like $\tilde{n}_e^2/n_e^2 \sim k_\perp^{-2}$. For larger values of $\tilde{n}_e^2/n_e^2$, the $\phi j_\parallel$ losses exceed the energy released in the volume, and fluctuations of this type attenuate.

According to the theory of turbulence with SD, the energy is transferred from shorter to longer waves and from poloidal to radial waves. In agreement with this, the steeper decrease of $\tilde{n}^2$ with increase of k, for k_θ and also for k_r Fig. 8, correlates with theoretical prediction. The limit of the variation of $S(k)$ is $k\rho_i \approx 0.1 - 0.15$, where ρ_i is the Larmor radius.

4.1.1. Enhanced radial correlations and diffusion for low plasma temperature

The simplest theoretical models predict SD in the SOL to be dominant if the inequality $\alpha = (m_e/m_i)^{1/2} L/\lambda_e \ll 1$ is fulfilled, where m_e and m_i are the electron and ion mass, respectively, L is the connection length, λ_e is the electron mean free path. The left side of this inequality is approximately equal to the inverse ratio of the product of the longitudinal electric field $E_\parallel$ and L to the Langmuir sheath potential $\approx T_e/e$ for floating conditions, i.e. it is the ratio of SD to volume dissipation by Coulomb collisions (VD). The inequality usually holds for tokamaks with small and middle sizes. However, for a cold, dense edge plasma, this inequality is not valid.

In TEXTOR-94 with connection length $L = 2\pi qR \approx$ 35 m, the parameter α is in the range 0–0.4 for the plasma conditions described above. For discharges with neon, this parameter is about 1–2. It means that VD is

comparable with SD. The radial correlation length is increased drastically with cooling by neon injection, the level of the density fluctuations and λ_n increase slowly.

The excitation of current-convective (rippling) turbulence in the presence of impurities in addition to SD is more likely to happen in this case. The reason of the turbulence is that the density fluctuations of low Z impurities in a dirty plasma result in Z_{eff} fluctuations, which in turn drive rippling instabilities. This possibility was discussed in [18,19]. Note, that under these conditions, the radial correlation length is comparable with the e-folding length of the density. Such large dimensions of the convection cells do agree with the theoretical estimation in the frame of impurity-driven rippling turbulence.

5. Conclusion

First measurements of electron density fluctuations, simultaneously resolved in radial and poloidal direction, have been made in TEXTOR-94 using the spectroscopical observations of two Li-beams. The radial correlation length in the SOL of TEXTOR-94 varies between 3 mm and 6 mm in plasmas with ohmic heating, and respectively between 7 mm and 13 mm with additional neutral beam heating. The measurements indicate that the poloidal correlation length is a factor of 3 to 4 higher than the radial correlation length. Outside the LCFS, the fluctuations propagate poloidally in the direction of the ion diamagnetic drift with a velocity of $\approx$1 km/s and their radial velocity is about $\approx$0.14 km/s inwards. Inside the LCFS, the fluctuations move in opposite direction, poloidally and radially. These propagation directions change sign with reversed magnetic field. The radial correlation length is increased with cooling by neon injection: $l_r \approx \lambda_n$ at radiation level of $\gamma \approx 0.8$, indicating a transition from surface dissipation to volume dissipation when the edge temperature is reduced.

Acknowledgements

The authors thank Ph. Mertens, G. Sergienko, G. Fuchs for fruitful discussions and the TEXTOR team for their support. One author has been supported by the Deutsche Forschungsgemeinschaft.

References

[1] S.J. Zweben, R.W. Gould, Nucl. Fusion 25 (1985) 171.
[2] M. Endler et al., Nucl. Fusion 35 (1995) 1307.
[3] M. Endler et al., Phys. Scr. 51 (1995) 610.
[4] A. Komori et al., Nucl. Fusion 28 (1988) 1460.
[5] B. Schweer, Atomic beams, in: Workshop on the Use of Atomic Beams in Plasma Experiments (Budapest 1993) KFKI-1993-19/D Report, 103.
[6] A. Pospieszczyk et al., Edge Diagnostic Using Atomic Beams, J. Nucl. Mater. 162–164 (1989) 574.
[7] H. Niedermeyer et al., Proceedings of the 18th Europ. Conf. on Controlled Fusion and Plasma Physics, Berlin, Germany, 1991, vol. 15C, Part 1, p. 301.
[8] A. Huber, PhD Thesis, Report Jül-3422 ISSN 0944-2952 (1997), Institut für Plasmaphysik, Jülich.
[9] A. Huber, U. Samm, B. Schweer, Method for simultaneous measurements of radial and poloidal components of fluctuation parameters using two thermal Li-beams, to be submitted to Nucl. Fusion.
[10] S. Coda, M. Porkolab, 24th Europ. Conf. on Controlled Fusion and Plasma Physics, Berchtesgaden, Germany, 1997, Vol. 21A, Part III, p. 1141.
[11] J. Boedo et al., J. Nucl. Mater. 196–198 (1992) 489.
[12] A.V. Nedospasov, J. Nucl. Mater. 196–198 (1992) 90.
[13] H. L. Berk et al., Nucl. Fusion 33 (1993) 263.
[14] X.Q. Xu, Phys. Fluids B5 (1993) 3641.
[15] R.N. Cohen, Contrib. Plasma Phys. 34 (1994) 232.
[16] V. Budaev et al., Plasma Phys. Contr. Fusion 35 (1993) 429.
[17] A.V. Nedospasov, M. Tokaŕ, in: B. Kadomtsev (Ed.), Problems of Plasma Physics, Vol. 18, Plenum Press (1994). Nucl. Fusion 220–222 (1995) 294.
[18] U. Samm et al., Plasma Phys. Rep. 22 (1996) 607.
[19] A.V. Nedospasov, Contrib. Plasma Phys. 36 (1996) 197.